Luhede, L., Wollborn, T. and Fritsching, U.

Stability of multiple emulsions under shear stress

Luhede, L., Wollborn, T. and Fritsching, U. (2020), Stability of multiple emulsions under shear stress. Can. J. Chem. Eng., 98: 186-193. https://doi.org/10.1002/cjce.23578

Stability of Multiple Emulsions under Shear Stress

Laura Luhede,[1,2]* Tobias Wollborn[2] and Udo Fritsching[1,2]

1. Research Training Group Mimenima, Bremen University, Bremen, Germany

2. Leibniz-Institute for Materials Engineering (IWT), Bremen, Germany

Multiple liquid emulsions of the water in oil in water ($W_1/O/W_2$) type are used in a variety of consumer or technical applications, for instance in the encapsulation of certain active ingredients. The encapsulation process and release mechanisms of the inner phase of the carrier drops are important in order to properly process and formulate such liquid-liquid systems. In this work the stability and breakage of multiple $W_1/O/W_2$ emulsions under mechanical shear stress are investigated for emulsions with different surfactants and surfactant concentrations of the internal emulsion. Stressing the emulsions in a mechanical stirring process is compared to the membrane emulsification process. The membrane emulsification process results in higher encapsulation efficiencies than the stirring process. The emulsion droplets were subjected to shear stress below and above the critical capillary number for drop breakup. The results show that stable inner emulsions with sufficient surfactant concentrations increase the overall encapsulation efficiency for multiple emulsions subjected to shear stress, although the effect is not prominent. The depletion of the carrier oil droplets could be achieved for Ca numbers below the critical limit, reducing the encapsulation efficiency below 10 %. This shows that even a low shear stress can result in content release from the internal droplet phase. The experimental emulsion release study is supported by a numerical simulation of drop deformation and break-up under shear stress.

Keywords: multiple emulsion, encapsulation, droplet breakup, emulsion stability, shear stress

INTRODUCTION

Multiple emulsions, ME, are complex multiphase structures that can be used for the encapsulation of active ingredients. Such liquid systems are of significant interest in the food, cosmetic, and pharmaceutical industries. The ability to encapsulate active molecules in the internal phase enables its potential application as a carrier system for drugs, the masking of flavors, or the encapsulation of ingredients such as vitamins.[1,2] Also, encapsulation can be used to protect the internal phase or exclude certain components, e.g., to reduce the fat content of a product.[3] The oil phase of a water in oil in water ($W_1/O/W_2$) emulsion acts as a liquid membrane separating the two aqueous phases. Thus, a potential sensitive medium is protected by an additional layer. Drugs and ingredients can be encapsulated in the carrier drop and the reactive component in the internal water phase can be released precisely where and when they are required. For the controlled release of ingredients and encapsulated substances, the analysis of the release mechanisms and the multiple emulsions stability are crucial.

Multiple emulsions are highly unstable systems as they consist of both water in oil (W_1/O) and oil in water (O/W_2) emulsions simultaneously. A lower osmotic pressure in the internal phase results in shrinking inner droplets, while a higher pressure makes the droplets swell. This is followed by film rupture of the oily carrier droplet, enabling the inner encapsulated droplets to escape. Therefore, it is essential to maintain a balance of the osmotic pressure to maintain stable multiple emulsions.[4,5]

The production and formulation of multiple emulsions generally requires a two-step emulsification process: first, the generation of the internal emulsion system (here, water in oil W_1/O); second, the emulsification of the W_1/O emulsion as the dispersed phase in a second aqueous phase (here named W_1/O in W_2).[6–9] Surfactants of low hydrophilic-lipophilic balance (HLB) are used to stabilize the internal emulsion, while high HLB surfactants are used for the outer emulsion. As this configuration is unstable and may break easily, the double emulsions are influenced by the application of stresses (chemical, mechanical, or thermal). Shearing causes droplet deformation and internal streaming flows in the droplets and the interfaces. This may increase the collision frequency of droplets, thus increasing coalescence rates. In addition, the droplet deformation changes the inner osmotic pressure. The droplets, for instance, elongate and increase the interface area available for encapsulated droplets to escape.[10] In several applications, emulsification methods where high shear stresses occur such as colloid mills, high pressure homogenization, and ultrasound are not applicable, especially for the second emulsification step.

Typical emulsification processes for the generation of multiple emulsions utilize a high shear method as first step. High energy input is required for the generation of small droplets in the oil phase. The second step requires less energy and shear forces. Conventional methods for the generation of the outer emulsion are stirring at low rotation speed or the drop generation through porous structures, such as, for instance, in membranes or microcapillaries.[7,11]

The use of membranes for the formulation of multiple emulsions enables a shear sensitive and controlled emulsification method. Membrane emulsification may generate high quality emulsions with narrow drop size distributions and high encapsulation efficiencies, depending on the membranes used. Various membrane emulsification processes have been developed

* *Author to whom correspondence may be addressed.*
E-mail address: l.luhede@iwt.uni-bremen.de
Can. J. Chem. Eng. 98:186–193, 2020

DOI 10.1002/cjce.23578
Published online 27 August 2019 in Wiley Online Library (wileyonlinelibrary.com).

for this purpose. Holdich et al.[12] developed a continuous membrane emulsification process with oscillatory flow, meaning the variation of the continuous phase velocity from the initial velocity to a maximum followed by a reduction back to the initial velocity. The advantage of the additional oscillation is an augmented instantaneous shear without increasing the continuous phase flow rate. Thus, the shear effect on the dispersed phase is increased. This setup provides opportunities to further process the generated emulsions, e.g., by spray drying the formed capsules. Dragosavac et al.[7] used a stirred cell membrane reactor for the creation of a crossflow for the support of droplet detachment through the rotation of a paddle stirrer. The use of flat disc membranes with laser cut pores enables the production of monodisperse emulsions at low pressure loss. In a review, Vladisavljević et al.[13] described various methods to produce ME in microcapillaries with multiple internal phases.

Hornig and Fritsching[14] investigated the premix membrane emulsification process for both spherical and non-spherical shaped sintered particle structures. They found that the porosity had a significant influence on the droplet size.

In several applications of multiple emulsions, a stable encapsulation or a controlled inner drop release is crucial. Particularly for controlled drug application, it is essential that reactives are not released before the destined area or time. Therefore, the study of multiple emulsion stability in flow conditions is of high importance.

The encapsulation efficiency (EE) describes the ratio of the encapsulated internal W_1 phase compared to the total amount of W_1 used in the emulsification process. A variety of different methods are available to determine the EE. Commonly, a marker is used in the internal phase to determine the release. Here, a straight forward method is the measurement of change in conductivity.[6–8,15,16] The marker is used in the W_1 phase and its concentration in the W_2 phase is measured after the emulsification process, determining the amount not encapsulated. The most common markers used are low-molecular-weight substances such as electrolytes, e.g., sodium chloride (NaCl),[8,15–17] or potassium chloride (KCl).[6] An actual extensive overview of analysis and measurement methods for EE is found in a review by Muschiolik and Dickinson.[18]

Schuch et al.[19] investigated the effect of the inner dispersed phase concentration on the stability and breakage of multiple emulsions. These authors visually examined the drop deformation and found that the application of shear stress has no influence on the drop collision rate of the internal emulsion drops. The deformation and relaxation time of the droplets was not influenced by the concentration of the internal phase.

The inner phase structure and its influence on drop breakup and internal phase release due to changes in the osmotic pressure was investigated by Neumann et al.[20] It was shown that diffusional processes occurring after droplet breakup significantly influence the drop size distribution.

Adsorption and desorption of surfactants and their effect on the visco-elastic behaviour of drops and interfaces can be determined by drop oscillation methods.[21,22] The viscosity is of crucial importance in the drop deformation and drop rupture process. The surface viscosity decreases the drop deformation and modifies the critical capillary number Ca_{crit} significantly.[23,24] Muguet et al.[25] showed that the higher the shear stress on a multiple emulsion, the higher the occurring release becomes.

In this contribution multiple emulsion stability against mechanical shear stress is analyzed by observing the encapsulation efficiency at different shear rates. Different surfactants and surfactant concentrations for the inner phase are used to modify the stability of the internal W_1/O emulsion. Thus, the influence of the stability of the W_1/O emulsion on the overall stability of multiple emulsion can be determined. The coalescence of the internal phase should occur for lower surfactant concentrations and may lead to an emulsion breakup,[4,5] which could be enhanced by the application of shear stress. The surfactant concentration of the outer emulsion is maintained constant. Therefore, only the effects appearing due to the influence of the internal phase are included in the analysis. A stirring process is used for the inner W_1/O emulsion. Two drop generation methods are compared for the generation of the outer emulsion, a membrane emulsification, and a stirring process, respectively. Thus, the influence of the drop generation mechanism can be evaluated.

MATERIALS

The $W_1/O/W_2$ emulsions were prepared using bi-distilled water for both aqueous phases and middle chain triglyceride (MCT) (Endima) for the oil phases. The viscosities are $\mu_{water} = 10^{-3}$ and $\mu_{oil} = 0.29\,kg\,m^{-1}\cdot s^{-1}$, respectively. As a marker for the evaluation of the encapsulation efficiency, NaCl (Sigma Aldrich) was used. A glucose monohydrate (Sigma Aldrich) solution was used to dilute the emulsion samples for conductivity measurements to determine the encapsulation efficiency.

The surfactants used were Tween 80 and sodium dodecyl sulphate (SDS) (Sigma Aldrich) as $W_1/O/W_2$ surfactants and Span 80 (Sigma Aldrich) for the W_1/O emulsion. The surfactant concentration range and properties are shown in Table 1. The surfactant concentration for the W_1/O emulsion was varied between $0.01–0.1\,g\cdot g^{-1}$ to generate emulsions with different internal stabilities. For the stabilization of the $W_1/O/W_2$ emulsion, the surfactant concentration of Tween 80 was chosen to be $0.005\,g\cdot g^{-1}$ (Table 1). This ensures that sufficient surfactant is present to properly stabilize the emulsion droplets.

The ratio of oil to water was 2:1 by mass for the W_1/O emulsion and 2:1 water to W_1/O emulsion for the double emulsion.

METHODS

For the quantitative evaluation of the double emulsion stability and breakage, an amount of $0.005\,g\cdot g^{-1}$ NaCl was added to the water phase of the W1/O emulsion as a marker of the inner phase. Figure 1 shows a schematic representation of a $W_1/O/W_2$ emulsion with the general encapsulation efficiency defined as follows:

$$EE = \frac{m_{W1}(t)}{m_{W1}(t_0)} \tag{1}$$

The W_1/O emulsion was created by stirring (Ultra Turrax T18/IKA) for 4 min at a rotational speed of 11 000 rpm.

The double emulsion systems were prepared by stirring and by membrane emulsification, respectively. For the first double emulsion, a magnetic stirrer (RH basic/IKA) was applied at 500 rpm for 10 min. For the membrane emulsification step, sintered particle

Table 1. Surfactant properties

Surfactant	HLB	CMC ($g\cdot L^{-1}$)	Concentration ($g\cdot g^{-1}$)
Span 80	4.3	-	0.01–0.10
Tween 80	15	$1.2\cdot10^{-5}$	0.005
SDS	40	$2.36\cdot10^{-3}$	0.0026

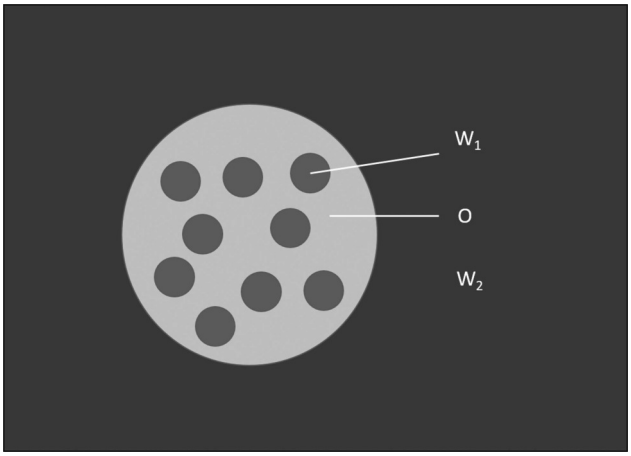

Figure 1. Scheme of $W_1/O/W_2$ emulsion.

glass membranes with an open porosity of 45 %, a thickness of 2.7 mm, and a mean pore size at 70 µm were used (ROBU, Germany). The pressure drop across the membrane was controlled to 50 kPa. The W_1/O emulsions were inserted in a container and then pressed at constant pressure through the membrane. To detach the droplets from the membrane, slow stirring by means of a blade stirrer within the product sampler was applied. All experiments were performed three times and a mean value with standard deviation was used for the results analysis. To gain a better understanding of the drop deformation process under shear conditions, a numerical multiphase flow simulation was performed for a single droplet in a shear flow. The solver interFoam of the open source CFD software OpenFOAM (Version 3.0) was used. The specific volume of fluid (VOF) method in OpenFOAM has an additional surface compression term:

$$\frac{\partial \alpha}{\partial t} + \nabla \cdot (\alpha U) + \nabla \cdot (\alpha (1 - \alpha) U_r = 0 \quad (2)$$

where α is the volume fraction; and U and U_r the velocity and relative velocity, respectively. The 3D simulation domain consisted of a rectangle geometry with $1.25 \times 2.5 \times 1.25\ m^3$ with periodic boundaries for inlet and outlet, moving wall boundaries at the upper and lower sides, and symmetry for the remaining patches. The computational cell geometry consists of a hex-mesh with an edge size of 12.5 µm resulting in a mesh with 2 m cells. The drop size investigated is 500 µm, corresponding to a volume of 0.065 µL. Grid independence and mass conservation have been monitored and ensured throughout the simulation runs.

MEASUREMENT

The drop size distribution in the emulsions was measured using laser diffraction (LA-960/Horiba). A suitable paste measurement cell (Horiba) was used for the inner W_1/O emulsion, while the drop size of the outer emulsion was measured using a fluid dispersion cell (Horiba).

The encapsulation efficiency was determined indirectly through the measurement of the electric conductivity (HI 20/PCE) in the emulsion. Therefore, the emulsion was diluted first in a glucose solution with bi-distilled water in a ratio of 1:20, thus decreasing the influence of the oil droplets on the conductivity.[5] The aim of this solution is the creation of the same osmotic pressure as in the inner water phase to avoid diffusion between the internal and the outer phase.[5,18,26]

The release of water is assumed to be proportional to the release of NaCl and can thus be calculated from the measured conductivity using a calibration curve. The calibration curve was derived to determine the encapsulation efficiency by adding a controlled NaCl quantity to an emulsion consisting of the same materials and concentrations as the multiple emulsion. An average of three independent measurements were used for the calibration curve.

Mechanical shear stress was applied on the double emulsion using a viscometer device (CVO 100/Bohlin) and shearing at defined shear rates of 50 .. 1500 s^{-1} in a cylindrical configuration. The shear rate is determined as follows:

$$\dot{\gamma} = \frac{\partial u}{\partial y} = \frac{\omega r_i}{\Delta h} \quad (3)$$

where $\Delta h = 1.25$ mm is the gap width; $r_i = 25$ mm is the inner diameter; and ω is the rotational velocity.

Drop size and emulsification efficiency were measured at several shear rate levels, where also a visual analysis of the emulsion systems by phase contrast microscopy (BX51/Olympus) was performed. The temporal stability of the emulsions was analyzed by turbidity measurements (TurbiScan LAB/Formulaction). The viscosities were measured using a rotary viscometer (CVO 100/Bohlin)

RESULTS

For the inner emulsion, different surfactant concentrations were used to prepare the basic W_1/O emulsion resulting in changing drop size distributions for each configuration. The drop size distributions in Figure 2 show an increase in the mean drop size for the lower surfactant concentrations. The standard deviation of drop size distribution between the different surfactant concentrations is below 0.02. Thus, the initial conditions concerning drop size can be assumed as constant. Turbidity measurements show that all multiple emulsions stay stable (the span of drop size distribution changes less than 5 %) for more than 4 h, which is the typical time required to perform the shearing experiments and the subsequent analyses.

Multiple emulsions are sensitive to shear stress due to their components. As shear is a main reason for emulsion breakup, it can be used to ensure a controllable release of content of the $W_1/O/W_2$ emulsion. By applying a defined shear stress on the multiple emulsions at known surfactant concentrations, the influence of the surfactant concentration on the encapsulation efficiency is to be determined. Premixing emulsification in sintered glass membranes with unstructured pores enable a reduction in droplet size distribution, which is shown in in Figure 2; the droplet size is 2–3 times the mean pore diameter, while, generally, a droplet size between 3–4 times are expected.

In Figure 3 the membrane emulsification method (M) is compared to the drop generation via stirring (S) for surfactant concentrations C = 1, 5, and 10 $g \cdot g^{-1}$ after being subjected to a defined shear stress. Data points are fitted using the Weibull function:

$$F(\dot{\gamma}) = 1 - e^{-(\dot{\gamma}/T)^m} \quad (4)$$

The accuracy is $R^2 = 0.88$ for M, 1 % and $R^2 > 0.96$ for the others. Here T represents the characteristic scale of the function and m

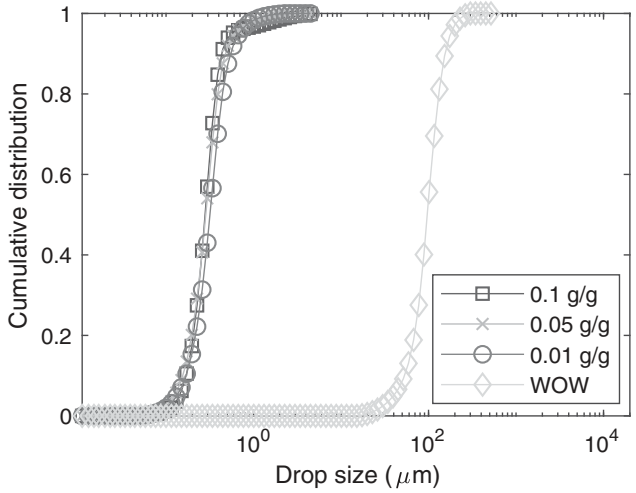

Figure 2. Drop size distribution of internal W_1/O emulsion for different surfactant concentrations (Span 80) with $W_1/O/W_2$ as comparison.

the slope of the function. The Weibull coefficients can be found in Table 2.

The slope of the graphs in the membrane emulsification process decreases with an increasing surfactant concentration C, with a rate of $y = 0.377 \ln(C)$. The graphs show that the initial encapsulation efficiency (shear rate = 0) is higher in the membrane encapsulation process (> 90 %) compared to stirring (~55 %). This also can be seen in the Weibull coefficients; In the stirring process the initial concentration is already low enough to generate a linear dependence with a rate of $y = 2.3725C - 1.3084$. This behaviour is due to the different drop generation mechanisms. Within the stirring process, the drops are broken through the application of shear and strain stresses. This rupture already may result in an unwanted release of the internal water phase content. The membrane emulsification process generates drops at the pore exit at the membrane surface by jetting or dripping.[27] The internal phase remains in the drop as there is no rupture of the interface. Low shear flow assists the drop detachment at the membrane surface.

The encapsulation efficiency, EE, decreases below 20 % for all surfactant concentrations for shear rates above 200 s^{-1}. Surfactants obviously have an effect on the encapsulation efficiency,

Table 2. Weibull coefficients

Emulsification process	m	T	R^2
M, 0.1 g/g	−1.4141	117.25	0.99
M, 0.05 g/g	−1.5166	83.20	0.96
M, 0.01 g/g	−2.2449	58.54	0.88
S, 0.1 g/g	−1.0691	25.88	0.91
S, 0.05 g/g	−1.1945	24.51	0.92
S, 0.01 g/g	−1.2821	12.99	0.93

however, the outer shear stress is dominant in the drop release process.

Figure 4 shows the drop size distribution for a 10 $g \cdot g^{-1}$ Span 80 multiple emulsion at different shear rates. Figure 4a shows that the drop size changes insignificantly for shear rates < 500 s^{-1}. For higher shear rates, the distribution becomes bi-modal as a fraction of smaller drops is generated. Figure 4b shows the drop size distribution at conditions of no shear and after shearing at 1500 s^{-1}. The drop size distribution shifts from a mono-modal function to a bi-modal function. A separate droplet population is created with $\bar{d}_{modal} \approx 25$ µm.

Thus, the typical breakage ratio in this case is as follows:

$$\epsilon = \frac{\bar{d}_{ini}}{\bar{d}_{1500}} \sim 5 \tag{5}$$

The Capillary number Ca is as follows:

$$Ca = \frac{\dot{\gamma}\,\eta\,d}{\sigma} \tag{6}$$

where $\dot{\gamma}$ represents the shear rate; η the viscosity; d the drop diameter; and σ the interfacial tension, which describes the fraction of disruptive stress to adhesive surface tension forces, thus giving a measure if a droplet remains stable under shear stress. Various authors assess the drop deformation and breakup mechanisms for clean interfaces.[24,28–31] The critical capillary number is defined for systems with low viscosity ratios $\lambda = \mu_D/\mu_C$. For $\lambda \gg 1$, as in O/W emulsions, the breakup criteria diverge. Here, drop breakup in pure shear flow is deemed impossible.[30]

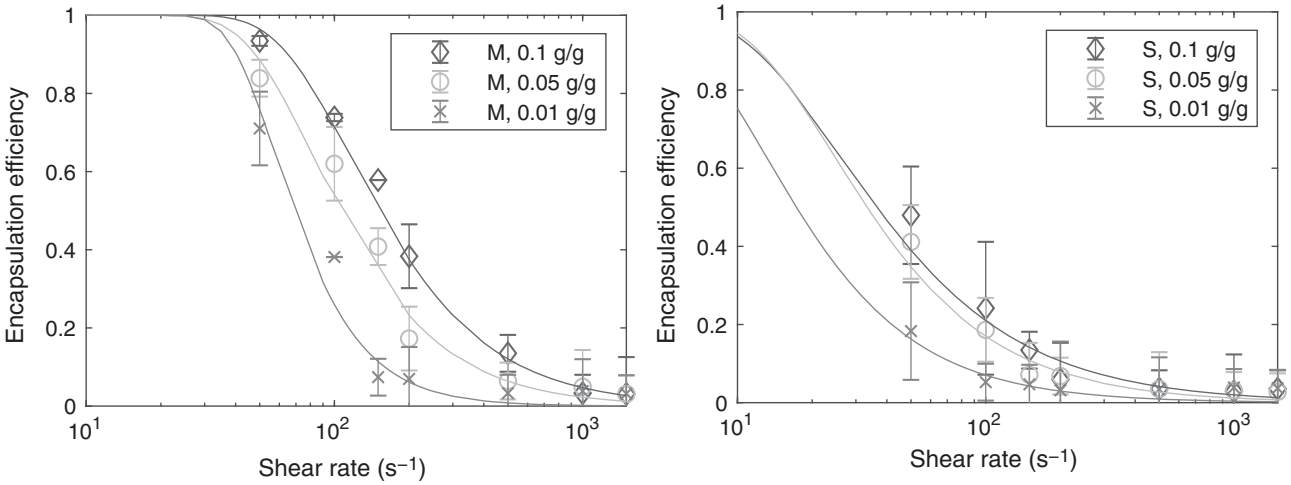

Figure 3. Encapsulation efficiencies, EE, for membrane emulsification (M), left, and stirring (S), right, process for different surfactant concentrations. Fitting with Weibull function with $R^2 > 0.88$.

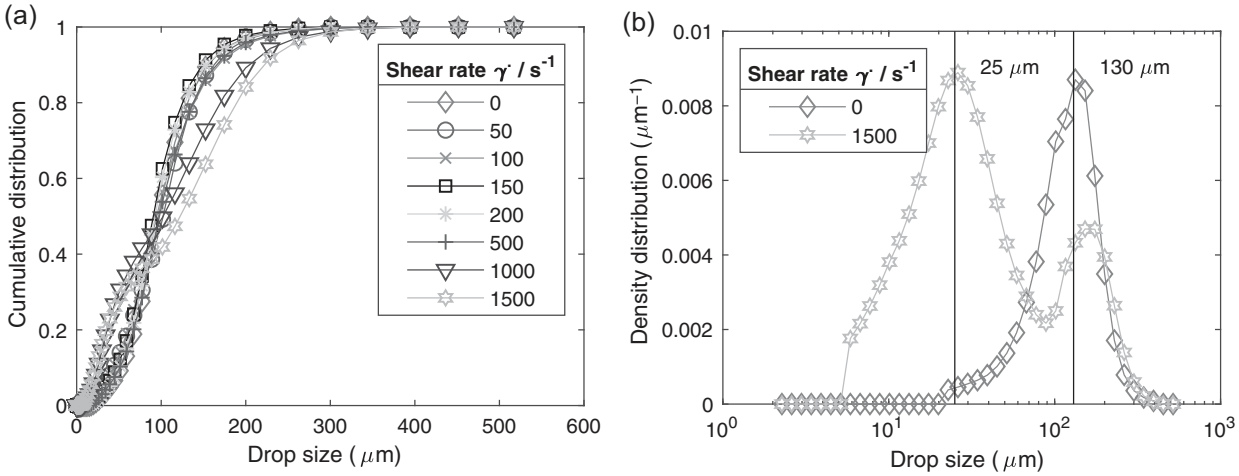

Figure 4. Drop size distribution of the membrane emulsification process (with 0.1 g · g^{-1} Span80) for: (a) various shear rates; and (b) before and after shearing at 1500 s^{-1}.

Numerical Simulation of Drop Deformation and Breakup

Figure 5 shows the drop deformation process for a shear rate of 1500 s^{-1} in combination with the velocity magnitude contours. In Figure 5a the interfacial tension corresponds to an almost clean interface that was measured using a pendent drop method (SCA25, DataPhysics). As can be observed, the droplet shape is nearly spherical despite the high shear stress. As the current system contains a high amount of surfactant, the actual interfacial tension is reduced. The measured final interfacial tension of the fully loaded interface is $\gamma = 0.0083$ kg·s^{-1} (SCA 25, DataPhysics). Applying the value from Figure 5c and an intermediate tension from Figure 5b to the simulation, the droplet deformation increases with a decreasing interfacial tension. Thus, a droplet breakup becomes possible for the loaded droplet case shown in Figure 5c.

The drop deformation for different capillary numbers ($\gamma = 0.0083$ kg·s^{-1}) is shown in Figure 6 in combination with velocity vectors at the outer side and inside of the droplet. Oil droplets in water are expected to maintain their shape for a high range of capillary numbers, showing only slight deformations. This corresponds with the findings in the literature.[24,30] The droplet rotates with the flow without deformation as indicated by the velocity vectors. Thus, the deformation depends less from the applied shear stress. However, a relation to the interfacial tension (Figure 5) is to be seen.

Derivation of Critical Capillary Number

In real emulsion systems, the drop deformation leads to surfactant concentration gradients on the droplet interface. The newly generated surface due to the shear and strain forces requires time before new surfactants can adsorb at the interface. The resulting Marangoni effect leads to a gradient in the interfacial tension, leaving parts of the droplet interface as a permeable membrane, which could lead to the release of inner droplets even before the actual drop rupture occurs. The presence of surfactants and the effect on the drop deformation was studied by Bazhlekov et al.[24] They found that the drop deformation depends linearly on the capillary number and that the drop deformation is very sensitive to the surfactant load on the interface. Still, the present simulation provides an estimate of

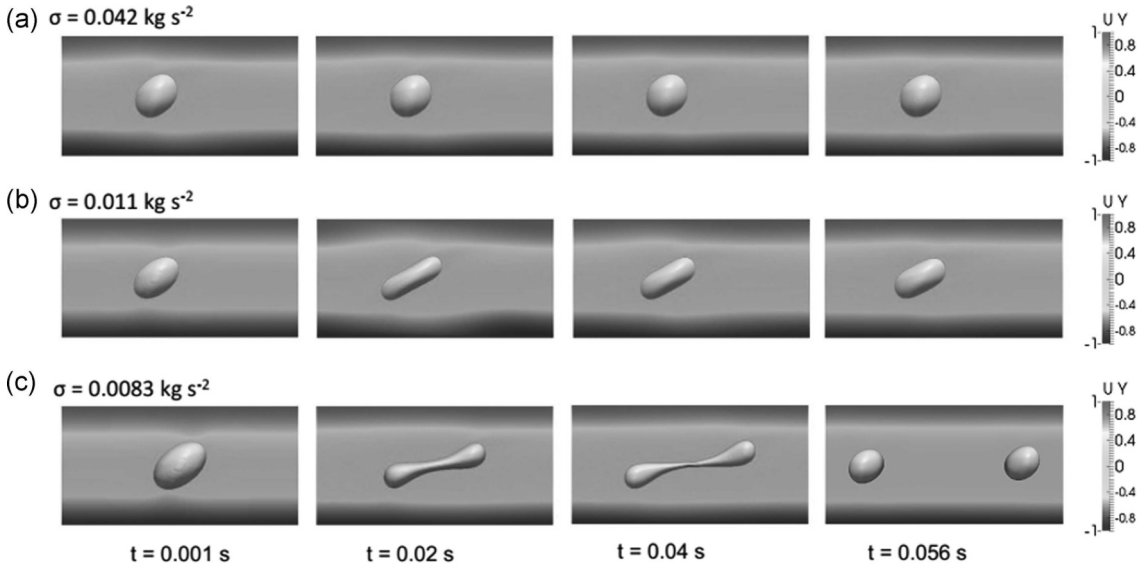

Figure 5. Simulation of drop in shear flow ($\dot{\gamma} = 1500$ s^{-1}) at a constant velocity for different interfacial tensions.

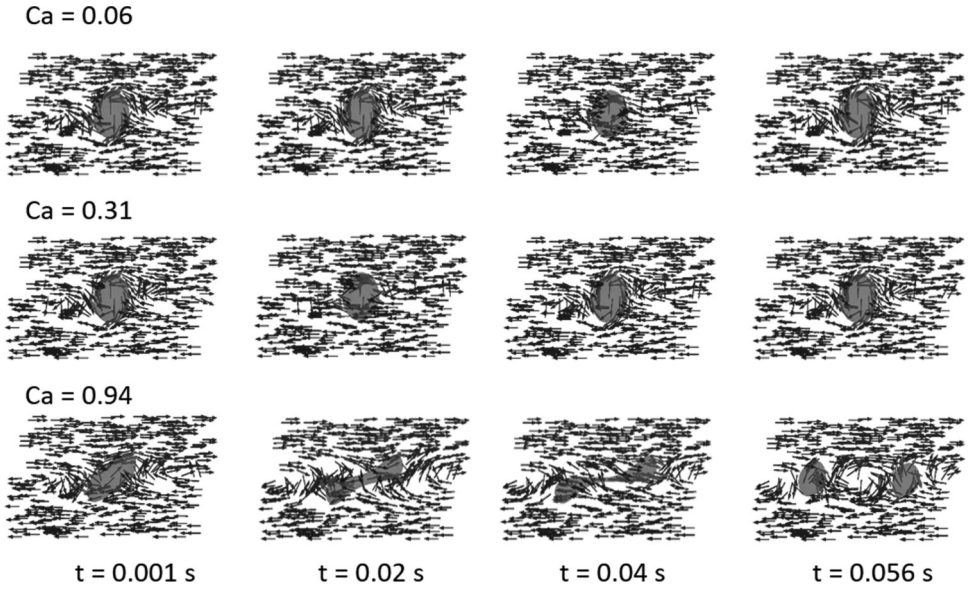

Figure 6. Drop deformation of 500 µm drop for rising capillary numbers. Red arrows show the velocity vectors for the dispersed phase inside the droplet, while arrows in blue identify the continuous outer phase.

the breakup of oil droplets in water and gives an approximate critical capillary number of $Ca_{crit} = 0.94$, which corresponds to the experimental data in Figure 7. Here, the capillary number that depends on the drop size is shown. This is also a strong indicator for the droplet depletion without drop breakup.

The release process of the inner aqueous phase can be monitored in microscopical images of the emulsion (Figure 8). Here, multiple emulsion samples have been stressed at constant shear rates for a defined time $\Delta t = 100$ s. The initial multiple emulsion is filled with small droplets. For increased shear rates, less encapsulated drops per phase appear, as well as completely depleted droplets.

The drop size however remains essentially constant. The fraction of empty drops increases as the shear stress rises. For a shear rate of $1500\,s^{-1}$ no filled droplets can be detected anymore. It also can be observed that for this shear rate the drops become smaller, as is already indicated by the measured drop size distributions (Figure 4).

Impact of Analysis Method on the Accuracy of Encapsulation Detection

The stability of multiple emulsions under shear or strain stress is influenced by several parameters such as the deformation rate, the drop diameter, and the viscosities of the dispersed and continuous phases.[25] The viscosity is influenced by the surfactants used. Tween 80 is a slowly absorbing surfactant. A faster surfactant should lead to increased encapsulation efficiencies in the same drop size regime. This tendency can be seen in Figure 9, where SDS (sodium dodecyl sulphate, Sigma Aldrich) was used as surfactant. The encapsulation efficiency increases significantly and independently from the applied shear rates. Here, the problem arises that using the same membrane emulsification process results in different drop size distributions due to the surfactant. As SDS produces much smaller drop size distributions for multiple emulsions, the results show a trend but no quantitative data regarding the exact effect of faster surfactants.

Whether the reduction in the encapsulation efficiency is due to the addition of NaCl as a marker needs to be further investigated. As described in the literature,[32–34] coalescence and flocculation increases with an increased salt concentration. However, previous work by Mezzenga et al.[5] indicates that for marker concentrations up to $0.5\,g\cdot g^{-1}$, the NaCl addition does not significantly influence the interactions at the drop interface. Unlike the present analysis, these multiple emulsions formulations have not been exposed to shear stress after the generation process. In Figure 10 the standard multiple emulsion prepared with a marker concentration of $0.5\,g\cdot g^{-1}$ is compared to a lower salt concentration of $0.1\,g\cdot g^{-1}$ NaCl. Sample emulsions also have been prepared with a NaCl concentrations of 1 and $0.8\,g\cdot g^{-1}$. In the latter cases, the emulsions immediately broke, making the analysis impossible. Figure 10 shows that lower marker concentration results in a slightly decreased release rate. It must be noted that for the low NaCl concentration ($0.1\,g\cdot g^{-1}$), the overall conductivity of the sample becomes lower, therefore increasing the uncertainty of the measurement results. Thus, the NaCl concentration used here has an almost negligible effect on the release of internal droplets as the rise in encapsulation efficiency is in range of the error bars. A more pronounced effect can be obtained by local concentration gradients of the internal phase. Due to droplet deformation, a former

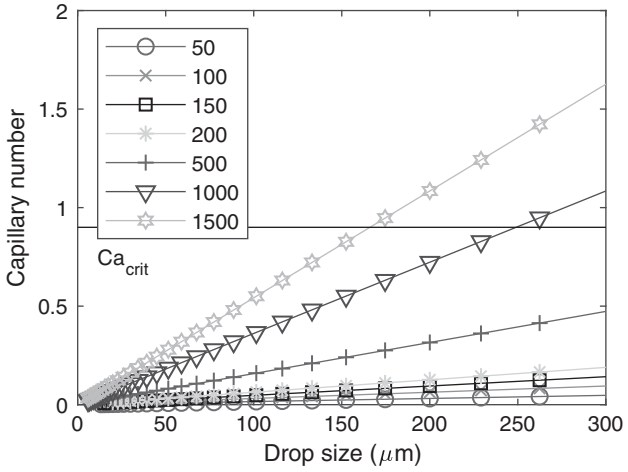

Figure 7. Capillary number versus drop size at different shear rates with Cacrit = 0.94.

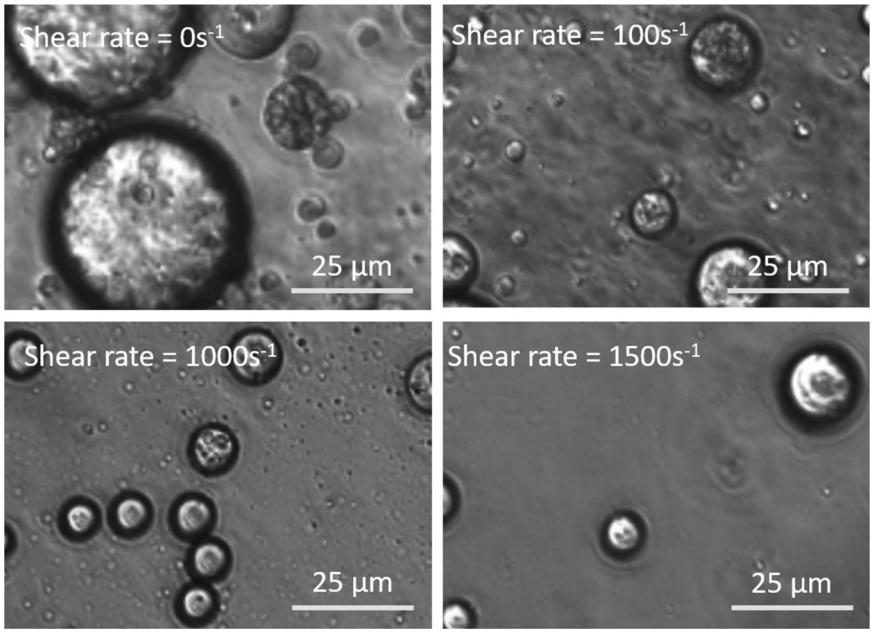

Figure 8. Optical microscopical images of multiple emulsions (membrane emulsification, surfactant concentration 0.1 g/g).

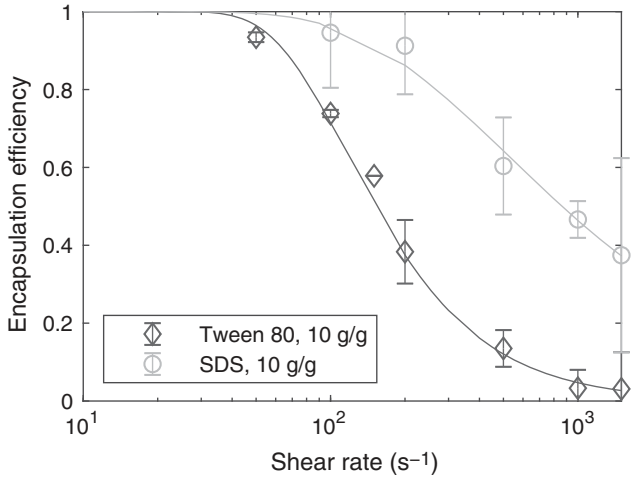

Figure 9. Comparison of the encapsulation efficiency with surfactants Tween 80 and SDS in the membrane emulsification process.

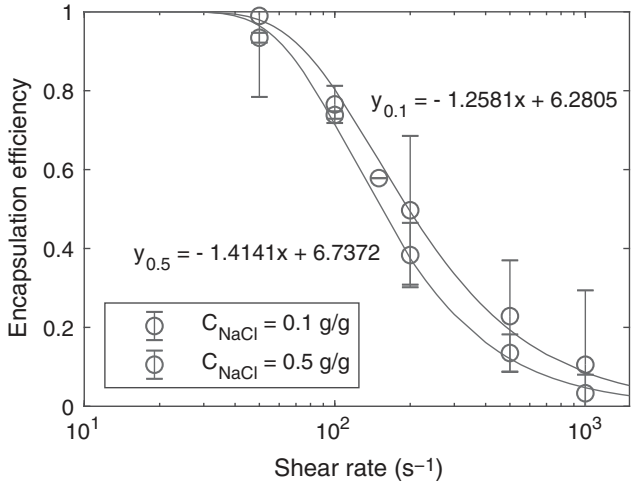

Figure 10. Encapsulation efficiency at different shear rates for marker concentrations 0.1 and 0.5 $g \cdot g^{-1}$ NaCl with 10 $g \cdot g^{-1}$ surfactant. Fitted by Weibull function with $R^2 > 0.977$.

homogenous droplet distribution can become heterogeneous. This effect may increase the collision frequencies of droplets leading to an increased coalescence rate, which increases with a decreasing surfactant concentration. The coalescence of internal droplets changes the osmotic pressure in the emulsion droplets, generating a permeable membrane in the oil droplet. The internal coalesced water droplets are more easily able to escape, leaving empty oil droplets.

CONCLUSIONS

The influence of shear stress on the stability of multiple emulsions ($W_1/O/W_2$) was analyzed. It was shown that even low shear stress results in a certain release of the encapsulated medium from the carrier droplet. This release is significantly influenced by the surfactant concentration of the W_1/O emulsion. Due to the increased stability of the internal emulsion, coalescence inside the carrier drop becomes less likely with a higher surfactant concentration, thus preventing the breakage of the emulsion.

Three interacting reasons for the multiple emulsion breakup are found. First, the shear forces acting on the droplet interface leads to deformation of the droplet, resulting in internal flow. During the shear process, the oil droplets are elongated and deformed. Surfactants molecules diffusion and adsorption on the O/W interface may be not fast enough to adapt to the geometrical change, thus generating a gradient in the surfactant concentration. The Marangoni effect leads to a partly permeable membrane on the interface, enabling the encapsulated drops to escape from the carrier drop. This release mechanism may even be enhanced by the NaCl concentration in the internal phase. A modification of the marker concentration results in slightly different

encapsulation efficiencies. The second reason for the emulsification breakup is the change in local concentration gradients that are leading to heterogeneous internal droplet distributions due to the drop deformation. This increases coalescence rates, depending on the surfactant concentration. The third reason is the coalescence of internal drops that change the osmotic pressure, generating permeable membranes and causing droplets to escape from the carrier drop.

Membrane emulsification is compared to a conventional stirring process for multiple emulsion formulation. The former process achieves much higher encapsulation efficiencies due to the specific low shear drop generation process. The encapsulation efficiency decreases in a similar way for both methods, indicating that the initial encapsulation efficiency is not relevant for the drop release process.

The internal drop release depends on a combination of shear stress, surfactant type, and concentration, as well as the surface properties of the media and drop size. The future development of a suitable correlation of these factors describing the emulsion stability under stress would provide a predictive method to determine a controlled release of internal phases in $W_1/O/W_2$ multiple emulsions.

ACKNOWLEDGEMENTS

This work was supported by the German Research Foundation (DFG) within the Research Training Group GRK 1860 "Micro-, Meso- and Macroporous Nonmetallic Materials: Fundamentals and Applications" (MIMENIMA) at the University of Bremen.

The authors thank the North-German Supercomputing Alliance (HLRN) for the HPC resources that contributed to the simulation results.

NOMENCLATURE

Ca	capillary number
CMC	critical micelle concentration
HLB	hydrophilic-lipophilic balance
MCT	middle chain triglyceride oil
ME	multiple emulsion
OW	oil in water emulsion
W_1/O	water in oil emulsion
$W_1/O/W_2$	water in oil in water emulsion

REFERENCES

[1] N. Garti, *Colloid. Surface.* **1997**, *124*, 233.

[2] N. Garti, A. Aserin, *Adv. Colloid Interfac.* **1996**, *65*, 37.

[3] J. E. Norton, I. T. Norton, *Roy. Soc. Ch.* **2010**, *6*, 3735.

[4] E. Dickinson, *Food Biophys.* **2011**, *6*, 1.

[5] R. Mezzenga, B. M. Folmer, E. Hughes, *Langmuir* **2004**, *20*, 3574.

[6] S. Frasch-Melnik, F. Spyropoulos, I. T. Norton, *J. Colloid Interf. Sci.* **2010**, *350*, 178.

[7] M. M. Dragosavac, R. G. Holdich, G. T. Vladisavljević, M. N. Sovilj, *J. Membrane Sci.* **2012**, *392–393*, 122.

[8] R. Lutz, A. Aserin, L. Wicker, N. Garti, *Colloid. Surface. B* **2009**, *72*, 121.

[9] M. Bonnet, M. Cansell, F. Placin, J. Monteil, M. Anton, F. Leal-Calderon, *Colloid. Surface. B* **2010**, *78*, 44.

[10] S. Van der Graaf, C. Schroen, R. Boom, *J. Membrane Sci.* **2005**, *251*, 7.

[11] U. Lambrich, H. Schubert, *J. Membrane Sci.* **2005**, *257*, 76.

[12] R. G. Holdich, M. M. Dragosavac, G. T. Vladisavljević, E. Piacentini, *Ind. Eng. Chem. Res.* **2013**, *52*, 507.

[13] G. Vladisavljević, R. Al Nuumani, S. Nabavi, *Micromachines* **2017**, *8*, 75.

[14] N. Hornig, U. Fritsching, *J. Membrane Sci.* **2016**, *514*, 574.

[15] Y. L. Kim, S. Mun, S. J. Rho, H. V. Do, Y. R. Kim, *Food Bioprocess Tech.* **2017**, *10*, 77.

[16] A. K. Pawlik, I. T. Norton, *J. Membrane Sci.* **2012**, *415–416*, 459.

[17] N. Chiu, L. Hewson, I. Fisk, B. Wolf, *Food Funct.* **2015**, *6*, 1373.

[18] G. Muschiolik, E. Dickinson, *Compr. Rev. Food Sci. F.* **2017**, *16*, 532.

[19] A. Schuch, L. G. Leal, H. P. Schuchmann, *Colloid. Surface. A* **2014**, *461*, 336.

[20] S. M. Neumann, I. Scherbej, U. S. van der Schaaf, H. P. Karbstein, *Colloid. Surface. A* **2018**, *538*, 56.

[21] F. Tamm, G. Sauer, M. Scampicchio, S. Drusch, *Food Hydrocolloid.* **2012**, *27*, 371.

[22] L. Luhede, F. Tamm, U. Fritsching, *Chem.-Ing.-Tech.* **2015**, *87*, 1109.

[23] J. Gounley, G. Boedec, M. Jaeger, M. Leonetti, *J. Fluid Mech.* **2016**, *791*, 464.

[24] I. B. Bazhlekov, P. D. Anderson, H. E. H. Meijer, *J. Colloid Interf. Sci.* **2006**, *298*, 369.

[25] V. Muguet, M. Seiller, G. Barratt, D. Clausse, J. P. Marty, J. L. Grossiord, *J. Colloid Interf. Sci.* **1999**, *218*, 335.

[26] A. Schuch, A. N. Tonay, K. Köhler, H. P. Schuchmann, *Can. J. Chem. Eng.* **2014**, *92*, 203.

[27] F. Krause, *Einfluss der Mikrofluidik beim Membranemulgieren*, PhD thesis, Universität Bremen, Bremen, Germany, **2012**.

[28] A. Acrivos, T. Lo, *J. Fluid Mech.* **1978**, *86*, 641.

[29] J. Li, Y. Renardy, *SIAM Rev.* **2000**, *42*, 417.

[30] H. P. Grace, *Chem. Eng. Commun.* **1982**, *14*, 225.

[31] M. Sellerberg, P. Walzel, *Chem.-Ing.-Tech.* **2010**, *82*, 1713.

[32] K. Demetriades, J. N. Coupland, D. J. McClements, *J. Food Sci.* **1997**, *62*, 342.

[33] B. Glasse, C. Assenhaimer, R. Guardani, U. Fritsching, *Can. J. Chem. Eng.* **2014**, *92*, 324.

[34] S. H. Mousavi, M. Ghadiri, M. Buckley, *Chem. Eng. Sci.* **2014**, *120*, 130.

Manuscript received September 27, 2018; revised manuscript received April 16, 2019; accepted for publication April 17, 2019.